

**FABRICATION OF MICRO-OPTICS FOR DIODE LASERS AND  
AMPLIFIERS USING INK-JET TECHNOLOGY**

**W. Royall Cox, Don J. Hayes, Ting Chen, Daryl Ussery, and Duncan MacFarlane**

**MicroFab Technologies, Inc.  
1104 Summit Ave, Suite 110  
Plano, TX 75074**

**March 1995**

**Final Report**

**APPROVED FOR PUBLIC RELEASE; DISTRIBUTION IS UNLIMITED.**

**19960828 052**

**PHILLIPS LABORATORY**



**PHILLIPS LABORATORY  
LASERS AND IMAGING DIRECTORATE  
AIR FORCE MATERIEL COMMAND  
KIRTLAND AIR FORCE BASE, NM 87117-577**

**PL-TR-95-1154**

Using Government drawings, specifications, or other data included in this document for any purpose other than Government procurement does not in any way obligate the U.S. Government. The fact that the Government formulated or supplied the drawings, specifications, or other data, does not license the holder or any other person or corporation; or convey any rights or permission to manufacture, use, or sell any patented invention that may relate to them.

This report has been reviewed by the Public Affairs Office and is releasable to the National Technical Information Service (NTIS). At NTIS, it will be available to the general public, including foreign nationals.


If you change your address, wish to be removed from this mailing list, or your organization no longer employs the addressee, please notify PL/LIDA, 3550 Aberdeen Ave SE, Kirtland AFB, NM 87117-5776.


Do not return copies of this report unless contractual obligations or notice on a specific document requires its return.

This report has been approved for publication.

  
CHARLES MOELLER  
Project Officer

**FOR THE COMMANDER**

  
NICHOLAS R. PCHELKIN, GM-15  
Chief, Semiconductor Laser Branch

  
ROBERT A. DURYEYEA, Colonel, USAF  
Director, Lasers and Imaging Directorate

REPORT DOCUMENTATION PAGE			Form Approved OMB No. 0704-0188	
Public reporting burden for this collection of information is estimated to average 1 hour per response, including the time for reviewing instructions, searching existing data sources, gathering and maintaining the data needed, and completing and reviewing the collection of information. Send comments regarding this burden estimate or any other aspect of this collection of information, including suggestions for reducing this burden, to Washington Headquarters Services, Directorate for Information Operations and Reports, 1215 Jefferson Davis Highway, Suite 1204, Arlington, VA 22202-4302, and to the Office of Management and Budget, Paperwork Reduction Project (0704-0188), Washington, DC 20503.				
1. AGENCY USE ONLY (Leave blank)	2. REPORT DATE March 95	3. REPORT TYPE AND DATES COVERED Final May 94 - Jan 95		
4. TITLE AND SUBTITLE FABRICATION OF MICRO-OPTICS FOR DIODE LASERS AND AMPLIFIERS USING INK-JET TECHNOLOGY			5. FUNDING NUMBERS C: F29601-94-C-0072 PE: 65502F PR: 3005 TA: CO WU: CJ	
6. AUTHOR(S) W. Royall Cox, Don J. Hayes, Ting Chen, Daryl Ussery and Duncan MacFarlane				
7. PERFORMING ORGANIZATION NAME(S) AND ADDRESS(ES) MicroFab Technologies, Inc. 1104 Summit Ave, Suite 110 Plano, Texas 75074			8. PERFORMING ORGANIZATION REPORT NUMBER	
9. SPONSORING / MONITORING AGENCY NAME(S) AND ADDRESS(ES) Phillips Laboratory 3550 Aberdeen Ave SE Kirtland AFB, NM 87117-5776			10. SPONSORING / MONITORING AGENCY REPORT NUMBER  PL-TR-95-1154	
11. SUPPLEMENTARY NOTES				
12a. DISTRIBUTION / AVAILABILITY STATEMENT  Approved for public release; distribution is unlimited			12b. DISTRIBUTION CODE	
13. ABSTRACT (Maximum 200 words)  Microjet printing methods were explored for in situ fabrication of micro-optical elements for use with diode laser and amplifier systems. Fabrication capabilities were demonstrated for hemispherical, hemielliptical and square microlenses, as small as 100 μm, with dimensional tolerances of better than 2 %. Microlenses were printed onto the tips of optical fibers, to increase their numerical apertures for light collection and with dye-diode formulations to create fluorescing, potentially lasing lenslet arrays. The optical material used ranged from optical adhesives dispensed at room temperature to optical resins and index-tuned thermoplastics printed at temperatures up to 200 °C. Data such as focal length and focal plane power distributions indicated that microjet printed microlenses were comparable or superior in optical performance to similar lenslets fabricated by conventional methods. This project demonstrated that microjet printing technology could significantly reduce the cost of micro-optics manufacture and that it can produce very fast (f/#, <f/2) hemispherical microlens arrays and unique hemielliptical lenslet arrays for diode laser array coupling and steering applications, neither of which can be fabricated cost effectively today by alternative state-of-the-art technologies.				
14. SUBJECT TERMS Micro-optics, microjet, ink-jet printing			15. NUMBER OF PAGES 30	
			16. PRICE CODE	
17. SECURITY CLASSIFICATION OF REPORT Unclassified	18. SECURITY CLASSIFICATION OF THIS PAGE Unclassified	19. SECURITY CLASSIFICATION OF ABSTRACT Unclassified	20. LIMITATION OF ABSTRACT SAR	

## PREFACE AND ACKNOWLEDGEMENTS

This report summarizes the results of a nine-month (SBIR Phase I plus Option Task) effort to explore the use of ink-jet printing methods for in situ fabrication of microlenses for potential use with diode lasers and amplifiers. The overall objective of this work was to assess the capability of this "Micro-optics Jet" technology, in order to determine its potential usefulness both for reducing the cost of fabrication of micro-optics and for providing new capabilities not currently available with current state-of-the-art alternative methods. The potential advantages of this "microjet" printing approach to micro-optics fabrication derive primarily from the fact that it is a low-cost (no photolithography), data-driven (computer controlled) process by which microlenses of various sizes and configurations may be printed directly onto optical substrates and components. Based on the results obtained on this project, a Phase II award was granted for developing specific micro-optics printing capabilities for applications of high interest to both the military and industrial sectors.

The authors would like to acknowledge the help of Dr. Ron Marusack of MicroFab for his work in setting up and programming the Micro-optics Printing Station, along with E. Wilson, V. Narayan and J.A. Tatum of the UTD Laser Lab for optical performance measurements of microjetted microlenses. Finally, we would like to extend our special appreciation for the helpful suggestions and technical guidance provided by Dr. Charles Moeller of Phillips Laboratories.

DTIC QUALITY INSPECTED 8

## CONTENTS

<u>Section</u>		<u>Page</u>
1.0	INTRODUCTION	1
1.1	PROJECT RATIONALE, OBJECTIVES AND STRATEGY	1
1.2	BACKGROUND: INK-JET PRINTING METHOD	2
1.3	ADAPTATION OF INK-JET METHOD TO MICRO-OPTICS PRINTING	3
2.0	EXPERIMENTAL METHODS	5
2.1	OPTICAL MATERIALS TESTING AND SELECTION	5
2.2	MICRO-OPTICS PRINTING SETUP & PROCESS	6
3.0	EXPERIMENTAL RESULTS	8
3.1	PRINTED MICROLENS ARRAYS	8
3.1.1	Spherical Microlens Arrays	8
3.1.2	Elliptical and Square Microlens Arrays	10
3.1.3	Fluorescing Microlenses	12
3.2	MICROLENSSES PRINTED ONTO OPTICAL FIBERS	13
3.3	OPTICAL QUALITY OF PRINTED MICROLENSSES	14
3.4	MICROLENS ARRAY BEAM STEERING EXPERIMENT	16
4.0	CONCLUSIONS	18
4.1	CAPABILITIES OF MICRO-OPTICS JET TECHNOLOGY	18
4.2	APPLICATIONS AND DEVELOPMENT CHALLENGES	18
	REFERENCES	20

## FIGURES

<u>Figure</u>		<u>Page</u>
1.	Schematic of drop-on-demand (DOD) ink-jet printing system.	3
2.	Generation of 50 $\mu\text{m}$ droplets of ethylene glycol by a DOD "microjet" device with a 50 $\mu\text{m}$ orifice at 2 kHz.	3
3.	Concept of micro-optics printing using ink-jet method.	4
4.	Hemispherical microlens diameter verses # of deposited microdrops.	4
5.	Optical material selection issues for microjet printing.	5
6.	Schematic of micro-optics jet printing station.	7
7.	Hemispherical microlens focal length and $f/\#$ verses diameter.	8
8.	Photograph and diffraction pattern of array of 100 $\mu\text{m}$ hemispherical, optical adhesive, microlenses on 125 $\mu\text{m}$ centers.	9
9.	SEM micrographs of array of 103 $\mu\text{m}$ hemishperical, optical thermoplastic microlenses printed on 115 $\mu\text{m}$ centers.	9
10	Photograph and diffraction pattern of array of 304 $\mu\text{m}$ x 196 $\mu\text{m}$ hemi-elliptical, thermoplastic microlenses.	10
11.	SEM micrographs of array of 381 $\mu\text{m}$ x 220 $\mu\text{m}$ hemi-elliptical microlenses.	11
12.	Printed square-shaped plano-convex, optical thermoplastic microlenses.	11
13.	Array of fluorescing hemispherical microlenses.	12
14.	Hemispherical microlenses printed onto the tips of 300 $\mu\text{m}$ optical fibers.	13
15.	Hemispherical microlenses printed onto the tips of 100 $\mu\text{m}$ optical fibers.	14
16.	Difference in power collection angle between unlensed and lensed 100 $\mu\text{m}$ fibers.	14
17.	Focal plane power distribution for optical adhesive microlenses.	15
18.	Focal plane power distribution for optical thermoplastic microlenses.	15
19.	Microlens array beam steering experimental setup.	16
20.	Beam steering angle verses array decenter distance.	17

## 1.0 INTRODUCTION

### 1.1 PROJECT RATIONALE, OBJECTIVES AND STRATEGY

Micro-optics, as an enabling technology for applications that cannot be addressed with conventional optics, is growing in importance for a wide range of state-of-the-art optical systems. Binary, or diffractive micro-optics have been developed for applications such as laser diode beam shaping,<sup>1</sup> beam splitting<sup>2</sup> and fill factor enhancement for focal plane imaging.<sup>3</sup> However, refractive microlenses offer an attractive, low-cost alternative in the case of short wavelength ( $\lambda < 1 \mu\text{m}$ ) systems requiring relatively high speed ( $< f/4$ ) lenslets<sup>4</sup>, e.g. in applications such as microlenses for increasing the efficiency of detector arrays<sup>5</sup> or imaging arrays for facsimile machines.<sup>6</sup> A commonly used method for fabricating refractive microlens arrays has involved the melting of photolithographically formed cylinders of photoresist,<sup>7</sup> where varying lenslet speed has been accomplished by preshaping of the cylinders by lateral mask translations<sup>8</sup> or laser machining.<sup>9</sup>

In this R&D project we have explored a new, low-cost technique derived from ink-jet printing technology for fabricating fast refractive microlenses and micro-optical interconnects. We have utilized this technology for the direct printing of optical materials in liquid form onto optical substrates and components to form plano-convex spherical or cylindrical microlenses. This method could offer both cost and flexibility advantages over photoresist cylinder melting processes in certain applications by enabling data-driven, in situ fabrication of micro-optical elements. For example, microlenses of differing sizes and speeds may be formed directly on an optical device, or on a substrate in an array at predetermined locations, as final value-added steps for system performance enhancement.

The broad goal in this work was to explore the potential capabilities of and advantages for using ink-jet printing methods for the fabrication and placement of both passive and active micro-

optical elements onto optical substrates and components, such as optical fiber tips and diode laser facets. The specific technical objectives of this R&D program included:

- (a) Determine several common optical materials, such as optical adhesives, resins and thermoplastics, which can be formulated for microjet printing by either heating or diluting with a solvent and precisely controlled in the printing and curing processes;
- (b) Develop microjet printing processes for variously sized and configured microlenses and microlens arrays and test them for optical performance;
- (c) Develop microjet printing processes for depositing microlenses onto the tips of optical fibers and active devices such as LED's and diode lasers;
- (d) Demonstrate the capability for printing elements of active optical materials.

The overall strategy for accomplishing these objectives was, firstly, to test for "microjetability," microdroplet formation and solidification/curing a wide variety of optical materials, in order to find several formulations to use in developing micro-optics printing processes. Secondly, those material formulations judged to be suitable for microlens printing by the microjetting process were utilized to determine the ranges of configurations and sizes of microlenses which could be microjet printed with sufficient precision to be useful in applications of high current interest. Thirdly, the microjet printed microlenses and lenslet arrays were optically characterized to determine their performance relative to similar optical elements fabricated by alternative state-of-the-art methods.

## 1.2 BACKGROUND: INK-JET PRINTING METHOD

Our micro-optics fabrication technique is based upon "drop-on-demand" (DOD) ink-jet printing, where a volumetric change in fluid within a print head is induced by the application of a voltage pulse to a piezoelectric transducer coupled to the fluid. This volumetric change causes pressure/velocity transients to occur in the fluid, and these are directed so as produce a drop that issues from an orifice.<sup>10</sup> In this type of printing system, depicted schematically in Figure 1, a voltage pulse is applied only when a drop is desired, as distinguished from the "continuous" type



where the print head produces a continuous stream of charged droplets which are directed to the target by deflection plates.<sup>11</sup> Since such systems are data-driven, single droplets or bursts of droplets ejected at frequencies up to 5 kHz may be printed at predetermined locations. The DOD microdroplet formation process is seen

in the photograph of Figure 2 which shows a print head tip generating 50  $\mu\text{m}$  diameter droplets under stroboscopic illumination at 2 kHz. Since the exposure time of this photograph was about 1 sec, the droplet images of Figure 2 are the superposition of about 2000 individual droplets, so the sharpness of these images indicates the extremely high level of size reproducibility, along with the spatial and temporal stability of microjetted droplets.

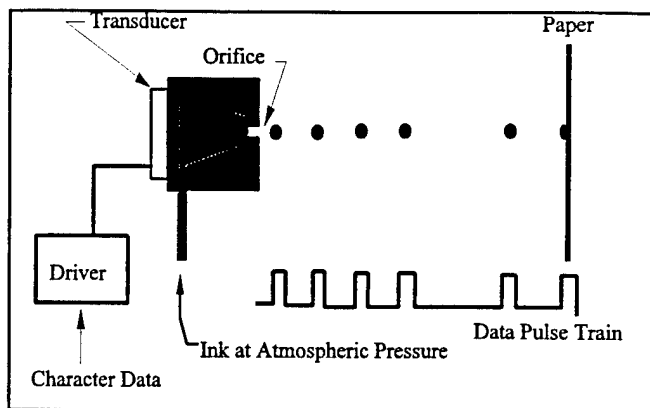


Figure 1. Schematic of a drop-on-demand ink-jet printing system.

In addition to traditional ink-jet printing, this "microjetting" method has also been used previously for such unconventional applications such as dispensing liquid solder for microelectronic packaging.<sup>12,13</sup>

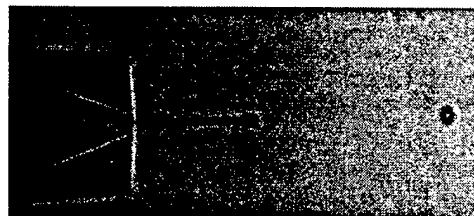


Figure 2. Generation of 50  $\mu\text{m}$  droplets of ethylene glycol at 2 kHz by a drop-on-demand "microjet" device with a 50  $\mu\text{m}$  orifice, where stroboscopically illuminated image is superposition of 2000 droplets.

### 1.3 ADAPTATION OF INK-JET METHOD TO MICRO-OPTICS PRINTING

If the ink and paper of this ink-jet system are replaced by an optical material and an optical substrate or component, respectively, and the system is provided with additional capabilities such as dispensing at elevated temperatures, it becomes a highly versatile tool for in situ micro-optics fabrication, as illustrated schematically in Figure 3.. The minimum feature size which

may be printed is determined by both the volume of the smallest ejectable microdroplet, as controlled by print head orifice diameter, and the degree of wettability of the substrate surface to the printed material. Single or multiple droplets printed onto a flat substrate spread and coalesce to form plano-convex elements upon solidification and/or curing.

Hemispherical lenslets of differing diameters and speeds are formed by varying:

- (a) the number of droplets per substrate site, as illustrated by the data of Figure 4,
- (b) substrate surface condition and
- (c) the type and/or solidification rate of the optical material used.

Other types of micro-optical structures, such as cylindrical/elliptical lenslets, microlens arrays and optical interconnects, may be printed by translating the substrate in the plane perpendicular to the jet and controlling its temperature.

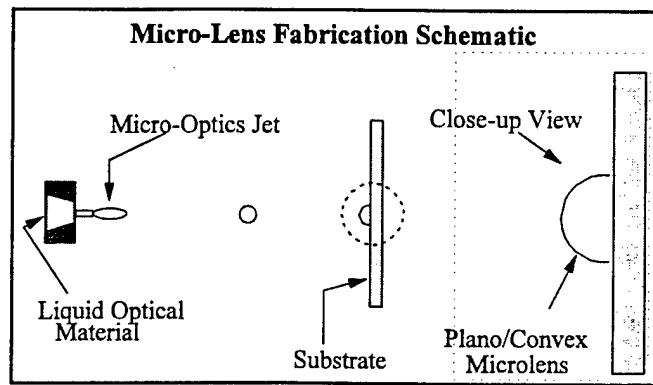


Figure 3. Concept of microlens fabrication by drop-on-demand ink-jet printing method.

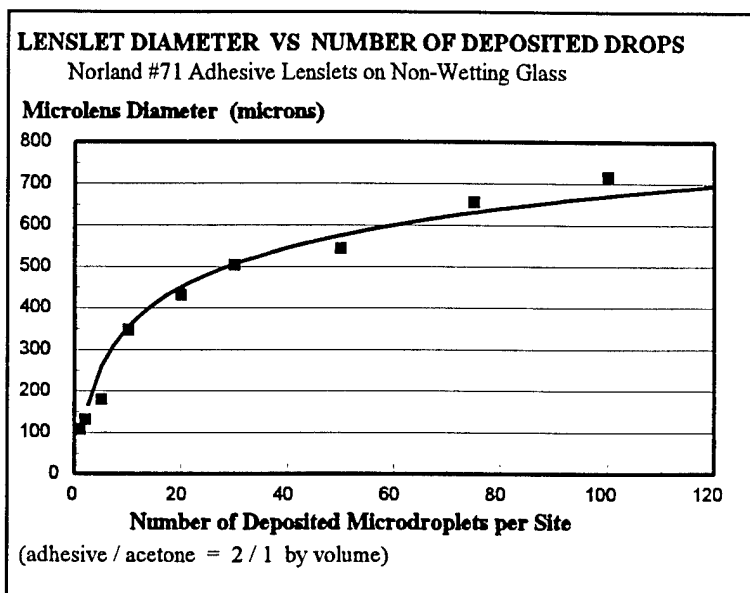


Figure 4. Hemispherical lenslet diameter as a function of the number of 50 μm diameter droplets microjet printed at a given lenslet site.

## 2.0 EXPERIMENTAL METHODS

### 2.1 OPTICAL MATERIALS TESTING AND SELECTION

Formulations of optical materials for microjet printing of micro-optics must satisfy two primary, sometimes contradictory, requirements. Firstly, after solidification and curing they should provide both the optical and physical properties needed for the particular application. Secondly, they must be reducible in viscosity below about 20 cps, by either heating or mixing with a solvent, in order to be readily printable by this method.

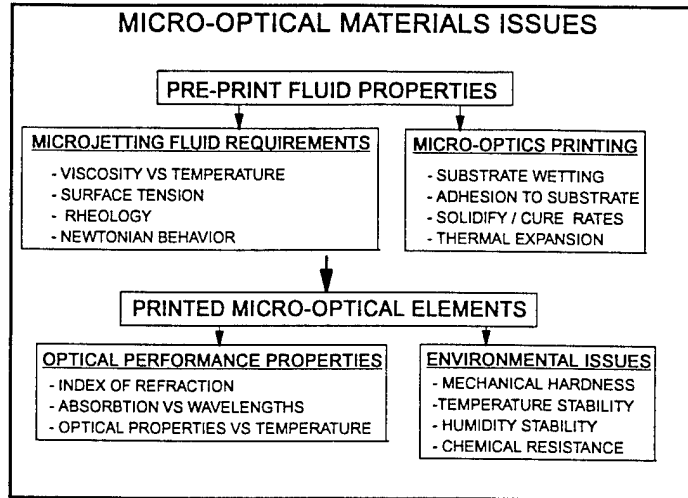


Figure 5. Issues involved in selecting and optimizing optical material formulations for microjet printing of micro-optical elements.

The various issues which must be considered in testing and selecting an optical material formulation for micro-optics printing range from its pre-print fluid properties to its post-print physical and optical performance characteristics, as indicated in Figure 5. The primary requirement for microjetting a material is that it be a homogeneous liquid of viscosity less than about 20 cps. Reduction of a potentially useful micro-optical material to this viscosity level is typically achieved either by raising its temperature or adding a "fugitive diluent" such as a solvent. Solvents are often employed for spin coating of photoresist onto substrates, for example, for subsequent microlens formation by polymer island melting. However, we found that evaporation of solvent from microjetted droplets during solidification can cause size and shape distortion in printed features, or that trapped solvent within the printed micro-optical element can inhibit the complete curing of the element. Therefore, solvent-free materials dispensed at elevated temperatures are inherently preferable for microjet printing.

A wide variety of off-the-shelf optical materials was examined for potential use in micro-optics printing, ranging from waxes, resins and organic polymers (e.g., acrylic photoreists) to UV-curing optical adhesives and catalytically activated epoxy formulations. Each candidate material was first measured for viscosity as a function of temperature or solvent concentration. Those for which the viscosity could be reduced to the required microjetting level, either by heating to within the 220°C upper limit of our microjet print head or by adding a determined amount of solvent, were then examined for macrodrop (1mm) formation, solidification and curing on glass substrates. Here a contact angle measuring goniometer with heated syringe dispenser was employed to observe the droplet formation and solidification process. Those optical material formulations which met both the viscosity and the uniform droplet formation and solidification criteria were then tested for microjet printing.

The types of micro-optical materials for which we have developed microjet printing processes to date include a variety of thermoplastics, such as index-tuned "meltmounts" and hydrocarbon resins dispensed at 100-200 °C, along with UV-curing, optical-adhesives/solvent formulations microjetted at room temperature.

## 2.2 MICRO-OPTICS PRINTING SETUP AND PROCESS

A schematic of our micro-optics printing station is pictured in Figure 6. The microjet print head, along with a 5 µm mesh stainless steel filter, is contained within a heating shell which is connected to a stainless steel heated fluid reservoir. All of the microjet printing parameters are set via the computer which controls both the function generator that provides the print head drive waveform and the XY-stage motion. A pulse generator, triggered by the function generator, drives an LED positioned below the print head orifice to provide stroboscopic illumination of the superimposed images of the ejected microdroplets during pre-printing, microjetting parameter optimization. The fluid reservoir, print head and target substrate are independently temperature-regulated in order to control fluid viscosity at the orifice and printed microdroplet solidification

rate.

The micro-optics printing process involves:

(i) adjusting print head temperature (up to 220°C) and drive waveform parameters to achieve stable microdroplet formation with the particular optical material to be printed,

(ii) setting the substrate surface condition and

temperature for optimal micro-optical element formation , then

(iii) specifying the specific pattern of print sites and the number of microdroplets to be printed per site.

Here substrate cleaning is obviously important and its surface may or may not be treated with a low-wetting coating to inhibit or encourage, respectively, droplet spreading and coalescence prior to solidification.

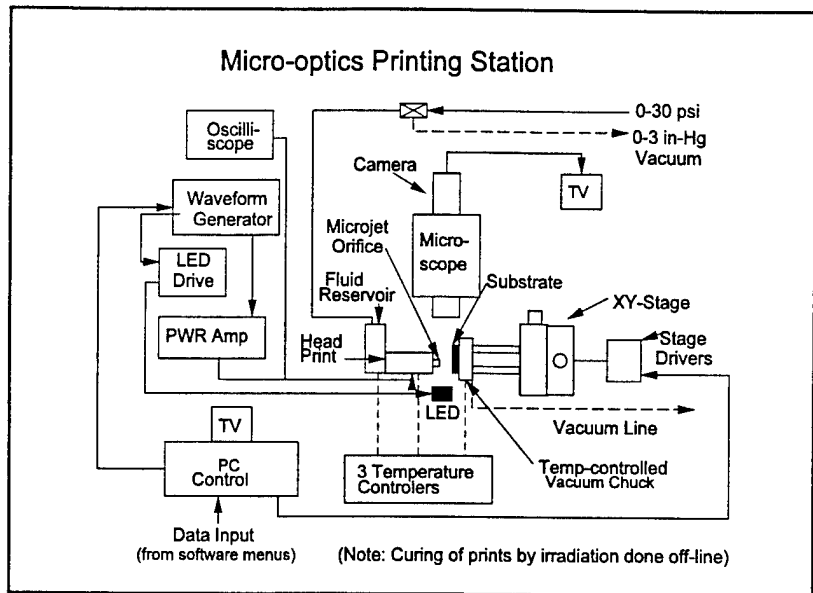


Figure 6. Schematic of micro-optics-jet printing station

### 3.0 EXPERIMENTAL RESULTS

#### 3.1 PRINTED MICROLENS ARRAYS

##### 3.1.1 Spherical Microlens Arrays

Arrays of plano-convex spherical (hemispherical) microlenses were fabricated by microjetting microdroplets of either optical-adhesive/solvent formulations at room temperature or optical thermoplastic materials at elevated temperatures onto optical substrates such as glass slides, and then solidifying the droplets by UV-curing or cooling, respectively. Here lenslet diameters are determined primarily by the size and number of microdroplets deposited. On the other hand, the speed ( $f/\# = \text{focal-length}/\text{diameter}$ ) of a microlens of a given diameter depends on the droplet surface tension and wettability of the substrate to the material being printed. This is illustrated in Figure 7 for the following cases: microlenses of low-index ( $n_D=1.53$ ) optical adhesive dispensed at 25°C onto (a) untreated glass

and (b) silicone-treated, low-wetting glass; (c) high-index ( $n_D=1.704$ ) thermoplastic "meltmount" lenslets, and (d) high-melting-point resin, dispensed at 145°C and 200°C, respectively. onto untreated glass. In all cases focal length varies linearly with diameter, whereas lenslet speed, as determined by line slope, varies independently of diameter with lenslet material and substrate surface condition (wetting

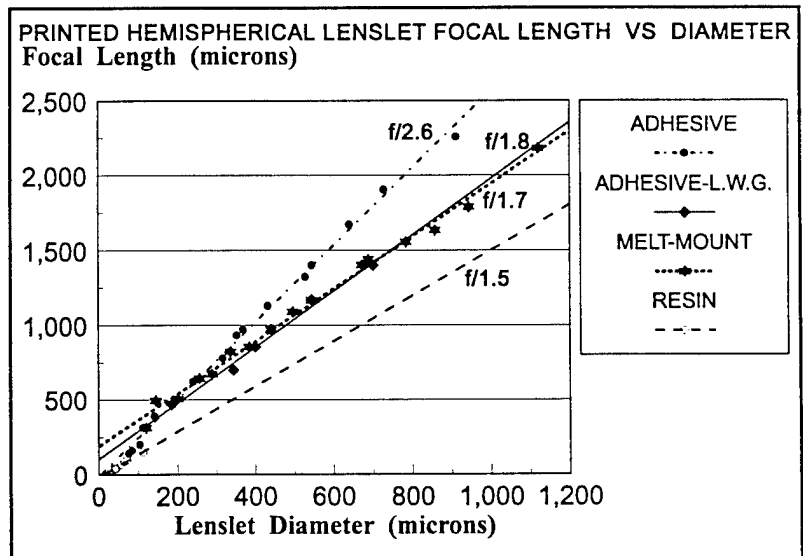


Figure 7. Variation of microlens  $f/\#$  & focal length with diameter, material and substrate condition for: optical adhesive printed at 25°C onto virgin & low-wetting surfaces and meltmount & resin at 145°C & 200°C, respectively.

verses non-wetting). Here lenslet speeds are seen to be variable by nearly a factor-of-two over the range  $f/1.5 - f/2.6$  by changing the microjetted material and substrate surface preparation, e.g., a 30% increase in speed can be obtained with the optical adhesive at a given lenslet volume by reducing the wettability of the glass.

Part of a typical array of such microlenses, along with its far-field-diffraction pattern under back-illumination with collimated light, is shown in Figure 8. Here a  $50 \times 50$  array of  $100 \mu\text{m}$  diameter lenslets on  $125 \mu\text{m}$  centers was printed onto a glass substrate treated with a silicone formulation for low surface wetting, by

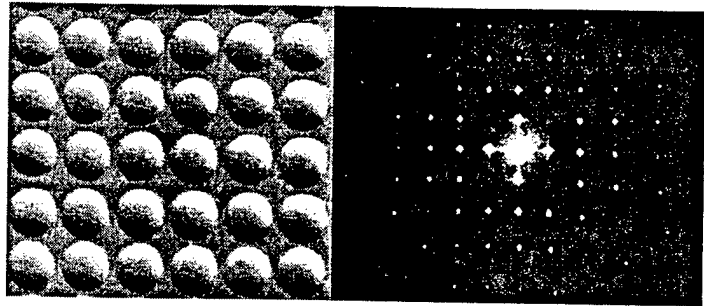


Figure 8. Optical micrograph and diffraction pattern of  $100 \mu\text{m}$  diameter plano-convex microlenses on  $125 \mu\text{m}$  centers, microjet printed with optical adhesive onto low-wetting glass.

dispensing  $50 \mu\text{m}$  droplets of a 2/1 mixture of Norland Products #71 optical adhesive and acetone at room temperature and then curing the structure under UV illumination. Microscopic measurements at 100X of lenslets selected at random over the entire array area indicated a standard deviation in diameter of  $2 \mu\text{m}$ . The uniformity and clarity of the diffraction pattern indicates good lenslet formation, optical quality and placement for this array.

Similar arrays of plano-convex spherical microlenses were fabricated by printing at elevated temperatures optical thermoplastic "meltmount" materials. Figure 9 shows SEM micrographs of part of an array of  $102 \mu\text{m}$  diameter,  $50 \mu\text{m}$  high lenslets on  $115 \mu\text{m}$  centers, created by microjetting at  $145^\circ\text{C}$  a high-index ( $n_D=1.704$ ) optical thermoplastic onto a glass substrate.. Assuming a spherical

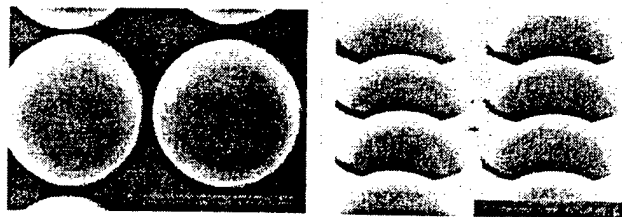


Figure 9. SEM micrographs of array of  $103 \mu\text{m}$  diameter,  $50 \mu\text{m}$  high, hemispherical microlenses printed on  $115 \mu\text{m}$  centers with high-index optical "meltmount" material at  $145^\circ\text{C}$  onto (untreated) glass substrates.

lenslet contour, these dimensional and index of refraction values give calculated values for focal length, speed and numerical aperture of  $73\ \mu\text{m}$ ,  $f/0.7$  and  $1.0$ , respectively. These data (though uncorrected for aberrations) clearly suggest that the microjet printing method can provide *significantly* "faster" microlenses than can be fabricated by any of the alternative state-of-the-art methods discussed above, thereby extending the range of potential applications of microlens arrays while simultaneously reducing the cost of manufacture.

### 3.1.2 Elliptical and Square Microlens Arrays

Plano-convex cylindrical/elliptical microlenses have been fabricated from the meltmount formulations by placing adjacent microdroplets at spacings which enable them to coalesce into a single elliptical droplet prior to solidification. Here the most critical process control parameters are substrate temperature (relative to the melting point of the microjetted material), droplet spacing on the substrate, and substrate surface condition (ideally clean and defect-free, but not non-wetting). Part of a  $20 \times 30$  array of cylindrical microlenses with corresponding diffraction pattern are pictured in Figure 10. Here each lenslet was formed by microjetting three each  $50\ \mu\text{m}$  droplets of 1.704 index meltmount at  $145^\circ\text{C}$  onto a glass substrate maintained at  $45^\circ\text{C}$ , at droplet-to-droplet spacings of  $75\ \mu\text{m}$ . These  $304\ \mu\text{m} \times 196\ \mu\text{m}$  microlenses are very reproducible, varying in major and minor axis dimension over the entire array by standard deviations of less than  $4\ \mu\text{m}$ . The overall size and length/width aspect ratio of these elliptical lenslets, along with placement positions, may be tailored by varying the printing process parameters to match a particular application or add value to an electro-optical device, e.g., to increase the efficiency of coupling the output of edge-emitting diode laser arrays to an optical fiber or the end of a solid-state laser rod. Again, the regularity and uniformity of the far-field diffraction pattern attests to the

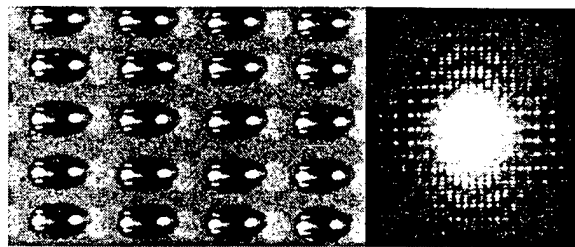


Figure 10. Hemi-cylindrical thermoplastic microlenses,  $304\ \mu\text{m} \times 196\ \mu\text{m}$ , printed at  $145^\circ\text{C}$  onto  $45^\circ\text{C}$  glass substrate, along with the diffraction pattern from  $20 \times 20$  lenslet array.



overall good optical quality of this particular array.

The major/minor axis ratio of such hemi-elliptical lenslets may be increased by increasing the number of adjacent droplets, as shown in the SEM micrographs of Figure 11, where four droplets were deposited on 65  $\mu\text{m}$  centers. As in the case of the hemispherical microlenses made from these meltmount materials, the SEM studies indicated smooth lenslet surfaces which appeared to be free of microstructure (other than the two small edge-cracks near the ends of the elliptical lenslets, which are attributed to the horizontal printing geometry and can be eliminated by going to a vertical jetting configuration).

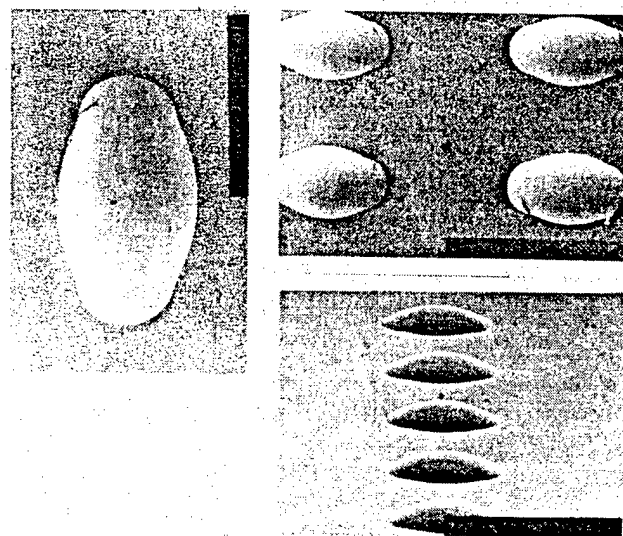


Figure 11. SEM micrographs (top photos viewed along and bottom one at 75° from surface normal) of array of hemi-elliptical microlenses, 381  $\mu\text{m}$ , 220  $\mu\text{m}$  and 106  $\mu\text{m}$  in length, width and height, respectively, fabricated by microjet printing of four adjacent 50  $\mu\text{m}$  droplets of high-index optical thermoplastic at 145°C onto 45°C glass.

By printing adjacent microdroplets of meltmount material along two dimensions in the substrate plane, square-shaped plano-convex microlenses with uniformly rounded tops were fabricated by essentially the same methods used for microjet printing hemi-elliptical lenslets. Examples of such micro-optical elements are given in the photographs of Figure 12. Here the nearly-square-shaped lenslets of the array were fabricated by

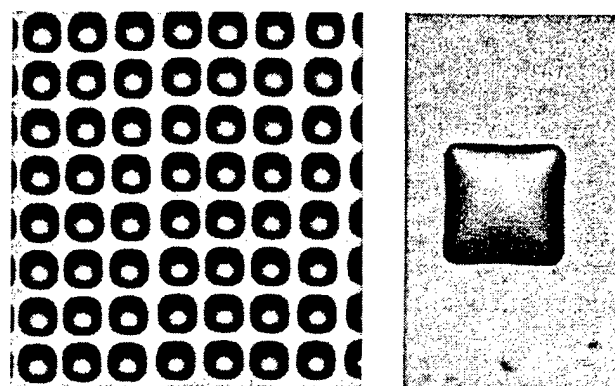


Figure 12. Array of 212  $\mu\text{m}$  wide square-shaped microlenses on 250  $\mu\text{m}$  centers (left) and a 630  $\mu\text{m}$  wide square lenslet (right)

printing a 3 x 3 matrix of adjacent 50  $\mu\text{m}$  droplets at each microlens site, while the single, larger square microlens was made by printing a similar 10 x 10 droplet pattern. In both cases the droplet center-to-center spacing for each microlens was 65  $\mu\text{m}$ . Obviously the more droplets used in a pattern the more nearly square the resultant microlens. Thus to microjet-print square lenslets on the order of 100  $\mu\text{m}$  wide would require a reduction in microjetted droplet size to about 25  $\mu\text{m}$  (which we have achieved with the optical adhesive material but not yet attempted with the thermoplastics). The potential value of such square-shaped microlenses would be to achieve higher array fill factors, e.g., for various imaging and scanning applications.

### 3.1.3 Fluorescing Microlens Arrays

As a demonstration of capability for microjetting *active* micro-optical elements onto optical substrates, the solvent used in the previously employed optical, UV-curing adhesive formulation was saturated with G6 Rhodamine dye prior to mixing with the adhesive in a 1/2 ratio. This material formulation was selected because the dye is totally miscible in the

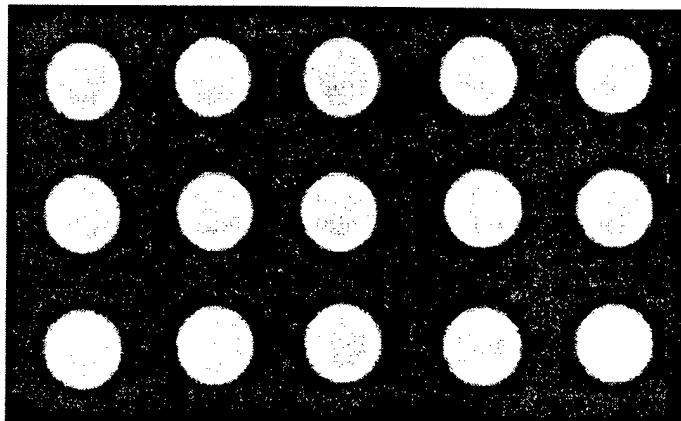


Figure 13. Array of 150  $\mu\text{m}$  diameter Rhodamine-doped adhesive lenslets fluorescing under UV illumination.

acetone/adhesive mixture and does not drop out of suspension over time. The mixture was then used to print an array of hemispherical, 150  $\mu\text{m}$  diameter lenslets on 200  $\mu\text{m}$  centers. Part of this microlens array is shown fluorescing under ultraviolet illumination in Figure 13. The next step in this direction would be to increase the dye concentration and optically pump the array from the back side with an argon laser to create in order to try to demonstrate an array of lasing microlenses. However, this was not pursued further because it did not fall within the mainline scope of this project, namely fabrication of micro-optics for diode laser and amplifier coupling.

### 3.2 MICROLENSSES PRINTED ONTO OPTICAL FIBERS

Experiments were conducted to explore the microjetting of lenslets onto the tips of optical fibers to optimize their numerical apertures for light collection applications. For this, a V-block fixture was fabricated and mounted on the XY stage to hold each target fiber with polished tip facing the print head orifice, at a distance of about 2mm.

As a first experiment, several polyimide-clad, 300  $\mu\text{m}$ -core multimode optical fibers were end-cut and polished prior to lenslet deposition. Visual alignment of each fiber tip to the 50  $\mu\text{m}$  print head orifice was initially achieved in the horizontal plane using the print-station microscope and in the vertical plane using an eye-loop magnifier. Fine tuning of the fiber position relative to the orifice was achieved during deposition of the

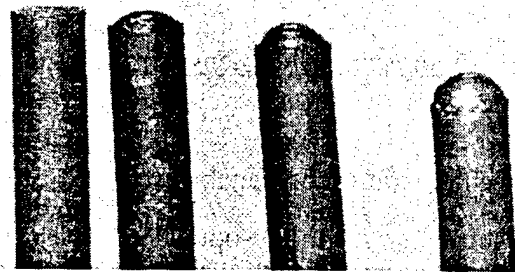


Figure 14. 300  $\mu\text{m}$  core, 340  $\mu\text{m}$  diameter glass optical fibers *without* (far left) and *with* optical adhesive, hemispherical lenslets, microjet printed at room temperature (with radii of curvature decreasing left-to-right).

lenslet by observing the impact location on the fiber face of ejected bursts of droplets and micropositioning the fiber to centralize the impact point. Adhesive formulation was microjetted onto the fiber faces in a series of manually triggered, 10-drop bursts. Since the outer edge of the fiber face effectively contains the spread of the deposited liquid, a wide range of lenslet radii of curvature were obtained by varying the amount of microdeposited material. This can be seen in the photograph of Figure 14 which shows three fibers with lenslet radii of curvature varying from about 300  $\mu\text{m}$  to 150  $\mu\text{m}$ , along with a fiber having only a polished tip. The number of 57  $\mu\text{m}$  diameter optical adhesive microdroplets ejected from the print head's 50  $\mu\text{m}$  diameter orifice, which were required to form these lenslets, ranged from 100 to 200.

In a second experiment we used the same visual alignment methods to print plano-convex

microlenses of high-index meltmount at 145°C onto the polished tips of 100 μm-core optical fibers with 20 μm thick cladding. The photograph of Figure 15 compares a bare polished tip to fiber tips having lenslets with four different radii of curvature, corresponding to 1,2,4 & 7 each 50 μm diameter droplets of deposited material.

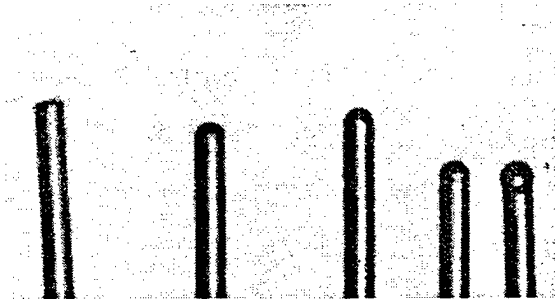


Figure 15. 100 μm optical fibers with (left-to-right) polished tip and tips with microjet printed lenslets of decreasing radii of curvature

Optical performance testing of these lensed fibers by scanning the cone of emitted light with a pinhole indicate that such microlenses on fibers of these dimensions increase (in comparison to fibers with only polished tips) the divergence angles of light coming out of the fibers, thereby increasing the effective numerical apertures for collection of light from highly divergent, multimode sources. As indicated in the polar plot data of Figure 16, this increase in collection angle can exceed a factor-of-two.

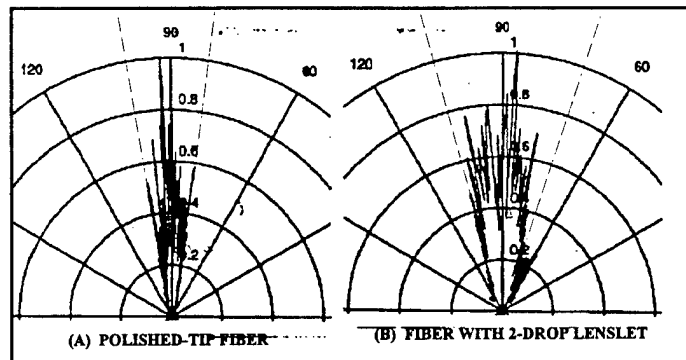


Figure 16. Comparison of divergence of light from bare fiber (A) and fiber with printed lenslet (B) made with two 50 μm droplets of optical thermoplastic (1st and 3rd fiber from left in Fig. 14., respectively).

### 3.3 OPTICAL QUALITY OF PRINTED MICROLENSES

An experiment was performed to compare the optical quality of the two material formulations we have been relying upon to date for most of our micro-optical element printing: the 2/1 Norland optical adhesive #71/acetone mixture, printed at room temperature and UV-cured off-line; and the Cargille Labs  $n_D=1.704$  meltmount printed at 145°C. To make this comparison two comparably sized hemi-spherical lenslets, one of each material, were selected and measured for

focal-plane point-spread power distribution. For these measurements a scanning pin hole setup was used in conjunction with a laser source and photodetector to measure the distribution of radiant power along a line in the focal plane through the center of each lenslet's focal spot. The resulting data for the meltmount and optical adhesive formulations are shown in Figures 17 and 18, respectively, where the same scale units in position and power were used for both scans. Here the most obvious difference between the data for these two lenslets is the peak width at half maximum (WHM), being 2.5X narrower for the meltmount microlens than for the optical adhesive one. This large difference in WHM value is especially significant considering the fact that a *narrower* peak would be expected for the optical adhesive lenslet based on the fact that its  $f/\#$  is 1.6X smaller, which would, for a similar diameter lenslet of the same material, give a much smaller spot size in the focal plane.

Consequently, these data indicate that the meltmount lenses are much more homogenous than the optical adhesive ones, probably due to the presence of residual solvent in the adhesive formulation which inhibits uniformity of curing. Given the greater flexibility of the meltmount material in micro-optical element formulation, provided by the lack of solvent and the ability to

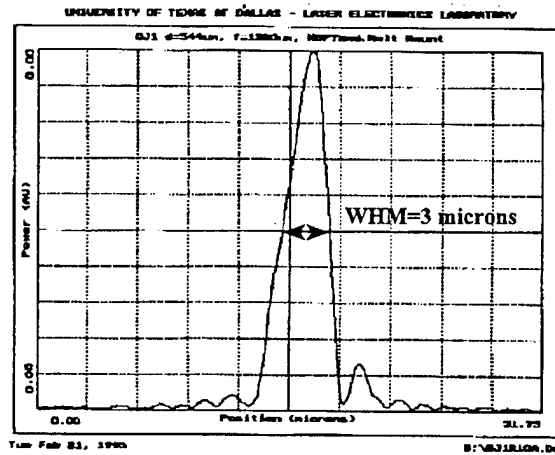


Figure 17. Power distribution in the focal plane of a microjet printed, high-index meltmount hemispherical microlens, 544  $\mu\text{m}$  diameter with 1200  $\mu\text{m}$  focal length ( $f/2.2$ ), where the X & Y axes are position(3  $\mu\text{m}/\text{div}$ ) and power (arbitrary units), respectively.

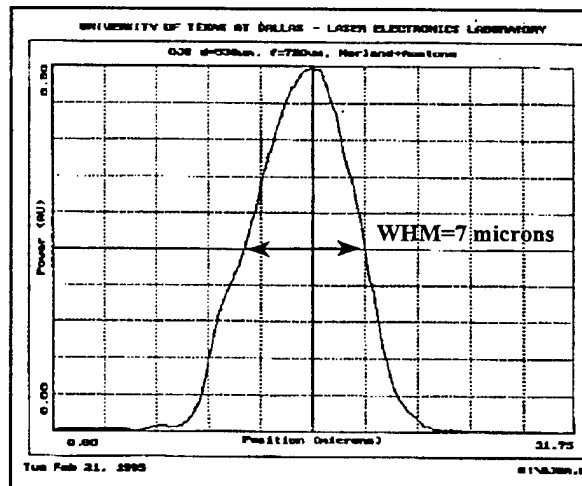


Figure 18. Power distribution in the focal plane of a microjet printed, high-index meltmount hemispherical microlens, 530  $\mu\text{m}$  diameter with 720  $\mu\text{m}$  focal length ( $f/1.4$ ), where the X & Y axes are position(3  $\mu\text{m}/\text{div}$ ) and power (arbitrary units of same scale as Figure 17), respectively.

control more precisely the coalescing and solidification of deposited microdroplets on the substrate, it is the current material of choice in our microjet printing of micro-optical elements.

### 3.4 MICROLENS ARRAY BEAM STEERING EXPERIMENT

Arrays of plano-convex microlenses, placed face-to-face, can be used for agile beam steering,<sup>14</sup> so a beam steering experiment using microjet printed optical adhesive microlens arrays was performed. In the experimental setup, illustrated in Figure 19, a HeNe laser beam was expanded by a factor of 30 and recollimated using a standard Galilean telescope. A micropositioner was utilized to set the spacing of two arrays, oriented face-to-face, equal to the sum of their focal lengths and to translate the second relative to the first in the transverse plane. Steering "agility" was obtained by measuring the displacement of the center of the far-field pattern as a function of array translation.

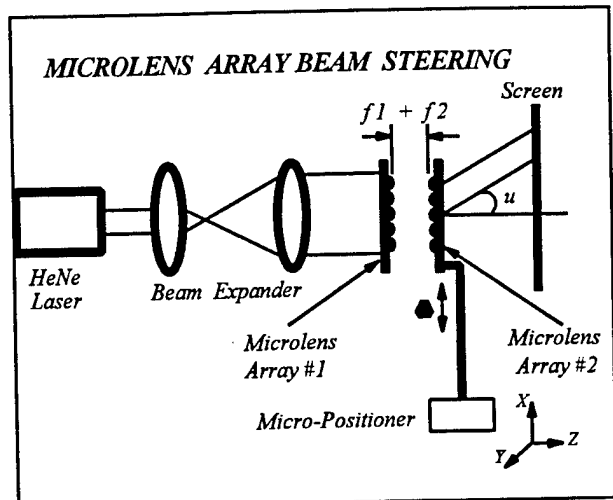


Figure 19. Beam steering by moving one microlens array relative (x-y) to another, with arrays positioned (z) at the sum of their focal lengths.

The 20 x 20 arrays consisted of spherical plano-convex lenslets, printed with UV-curing optical adhesive on 700  $\mu\text{m}$  centers onto low-wetting glass substrates. The lenses of the first array in the optical path were 530  $\mu\text{m}$  in diameter and had a focal length of 720  $\mu\text{m}$ . Two arrays were used in the scanner position having lenslet diameter & focal length of 530  $\mu\text{m}$  & 800  $\mu\text{m}$  and 440  $\mu\text{m}$  & 540  $\mu\text{m}$ , respectively. The data for these two configurations, shown in Figure 20, are seen to follow the expected governing relationship among the scan angle  $u$ , the focal length  $f_2$  of the decentered array and the decenter distance  $\Delta$ :

$$\tan(u) = \frac{\Delta}{f2}$$

Here it can be seen that an array of fast (f/1.2) 500 μm focal length lenses decentered by only 100 μm produces a scan angle of 11 degrees. A total scan angle of about 40 degrees was achieved with a nearly linear relationship between steering angle and array decenter (though the scanned beam focal quality degrades, as expected in the less linear regions).

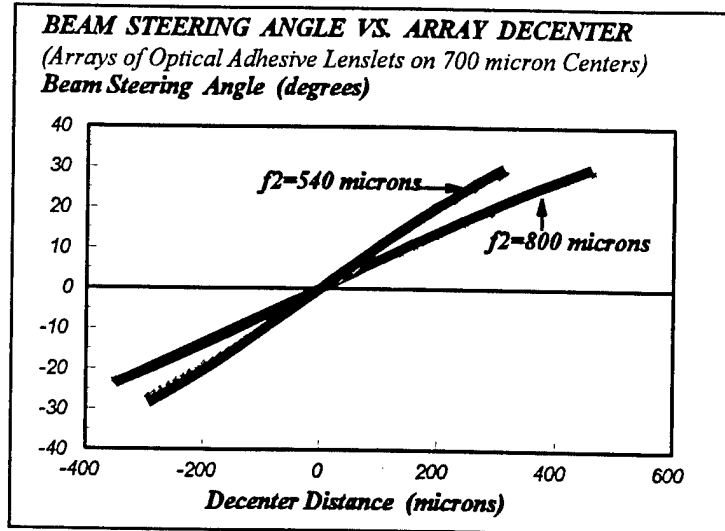


Figure 20. Beam steering angle as a function of array decenter distance for two printed microlens arrays and two focal lengths for the second array.

## 4.0 CONCLUSIONS

### 4.1 DEMONSTRATED CAPABILITIES OF MICRO-OPTICS JET TECHNOLOGY

The following conclusions may be drawn from the results of our R&D work to date:

(a) Microjet printing *is* a very feasible approach for the fabrication of a variety of refractive micro-optical elements;

(b) This method is capable of forming potentially important micro-optical elements, such as hemi-elliptical and very-fast-hemispherical microlenses (of dimensional reproducibilities better than 2%) which cannot be fabricated as cost effectively today by alternative technologies;

(c) Micro-Optics Jet technology appears to offer the potential for reducing significantly the cost of manufacture many optoelectronic systems, such as fiber-coupled diode laser arrays, by providing, primary or corrective optics in situ, as a value-added step in the system manufacturing process.

(d) As a highly-flexible, totally data-driven process Micro-Optics Jet technology provides completely new capabilities for micro-optics manufacture, such as printing arrays of microlenses of differing configurations, aspect ratios and indices of refraction on the same optical substrate or component.

### 4.2 APPLICATION AND DEVELOPMENT CHALLENGES

The number of specific optoelectronic system manufacturing applications for which this Micro-Optics Jet technology could potentially provide significant benefits depends, of course, on the specific micro-optics printing capabilities which are ultimately achieved. Improvement of these capabilities, which constitutes the key challenge for future development during the Phase II work, involves the following three development areas:

(i) *Micro-optical materials development for microjet printing:*

The optical material formulations used for microjet printing will have to be more environmentally stable and durable than the ones employed during the Phase I effort, in order to



be usable in most practical applications, such as the coupling of power diode laser outputs to optical fibers. Here the challenge will be to develop formulations of more stable materials, involving, for example, state-of-the-art optical organic polymers, which may be microjet printed at temperatures less than the current 220°C limitation of our print head device and solidified and cured without anisotropic distortion or shrinkage.

*(ii) Micro-droplet placement precision:*

The precision of droplet placement on optical substrates will need to be improved to achieve the lenslet-to-lenslet spacing accuracy required for sensitive beam steering applications. We have demonstrated the capability for forming arrays of various configurations of microlenses on the order of 100-200  $\mu\text{m}$  in size to dimensional tolerances of 1-2 %. However, the accuracy of lenslet placement on optical substrates and components will need to be improved substantially for applications such as diode laser beam steering, where lenslet-to-lenslet spacings of +/- 1-2  $\mu\text{m}$  are required.

*(iii) Reduction in minimum printable micro-optical feature size:*

With our current microjet materials, methods and hardware we have demonstrated the capability for reliable printing of lenslets as small as 70  $\mu\text{m}$ , which will be adequate for most diode laser beam steering and shaping applications. By reducing this minimum printable micro-optical feature size to the 20  $\mu\text{m}$  level we would be able also to address with this technology microlens arrays for optical scanning, CCD (charge-coupled device) and FPD (flat panel display) applications .

## REFERENCES

(All portions of this list of references are UNCLASSIFIED)

1. Veldkamp, W.B., "Laser beam profile shaping with interlaced binary diffraction gratings," Appl. Opt., Vol 21, pp. 3209-3212, 1982.
2. Streibl, N., U. Nolscher, J. Jahns and S. Walker" Appl. Opt., Vol. 30, No. 19, pp. 2739-2742, 1991.
3. Motamedi, M.E., W.H. Southwell, R.J. Anderson, W.J. Gunning and M. Holz, "High speed binary microlens in GaAs," Proc. SPIE, Vol. 1544, pp. 33-44, 1991.
4. Motamedi, M.E., "Micro-opto-electro-mechanical systems," Opt. Eng., Vol. 33, No. 11, pp. 3505-3517, 1994.
5. Farn, M.W., "Micro-concentrators for focal plane arrays," in Miniature and Micro-Optics: Fabrication and Systems Applications II, Proc. SPIE, Vol. 1751, pp. 106-117, 1992.
6. Bellman, R.H., N.F. Borrelli, L.G. Mann and J.M. Quintal, "Fabrication and performance of a one-to-one erect imaging microlens array for fax," in Miniature and Micro-Optics: Fabrication and System Applications, Proc. SPIE, Vol. 1544, pp. 209-217, 1991.
7. Popovic, Z.D., R.A. Sprague and G.A. Neville Connell, "Technique for monolithic fabrication of microlens arrays," Appl. Opt., Vol. 27, pp. 1281-1284, 1988.
8. Daly, D., R.F. Stevens, M.C. Hutley and N. Davies, "The manufacture of microlenses by melting photoresist," Meas. Sci. & Techn. Vol. 1, pp. 759-766, 1990.
9. Jay, T.R. and M.B. Stern, "Preshaping photoresist for refractive microlens fabrication," Opt. Eng., Vol. 33, No. 11, pp. 3552-3555, 1994.
10. Bogy, D.B. and F.E. Talke, "Experimental and theoretical study of wave propagation phenomena in drop-on-demand ink jet devices," IBM Journ. Res. Dev., Vol. 29, pp. 314-321, 1984.
11. Pimbly, W.P., "Drop formation from a liquid jet: a linear one-dimensional analysis considered as a boundary value problem," IBM Journ. Res. Dev., Vol. 29, p. 148, 1984.
12. Hayes, D.J., D.B. Wallace, M.T. Boldman and R.M. Marusak, "Picoliter solder droplet dispensing," Microelectronics and Electronic Packaging, Vol 16, pp. 173-180, 1993.
13. Iverson, W.R., "Liquid solder jetting attracts U.S. research," Assembly Magazine, pp.27-30, March, 1994.
14. Watson, E.A., "Analysis of beam steering with decentered microlens arrays," Opt. Eng., Vol. 32, pp. 2665-2670, 1993.

## DISTRIBUTION LIST

AUL/LSE  
Bldg 1405 - 600 Chennault Circle  
Maxwell, AFB, AL 36112-6424 1 cy

DTIC/OCP  
8725 John J. Kingman Road, Suite 0944  
Ft Belvoir, VA 22060-6218 2 cys

AFSAA/SAI  
1580 Air Force Pentagon  
Washington, DC 20330-1580 1 cy

PL/SUL  
Kirtland AFB, NM 87117-5776 2 cys

PL/HO  
Kirtland AFB, NM 87117-5776 1 cy

Official Record Copy  
PL/LIDA  
Charles Moeller 2 cys

MicroFab Technologies, Inc.  
1104 Summit Ave, Suite 110  
Plano, TX 75074 1 cy